Characterization of aperiodic and periodic thin Cu films formed on the five-fold surface of *i*-$Al_{70}Pd_{21}Mn_9$ using medium-energy ion scattering spectroscopy

J. A. Smerdon, J. Ledieu,* and R. McGrath
Surface Science Research Centre, The University of Liverpool, Liverpool L69 3BX, United Kingdom

T. C. Q. Noakes and P. Bailey
CCLRC Daresbury Laboratory, Daresbury, Warrington WA4 4AD, United Kingdom

M. Draxler and C. F. McConville
Department of Physics, University of Warwick, Coventry CV4 7AL, United Kingdom

T. A. Lograsso and A. R. Ross
Ames Laboratory, Iowa State University, Ames, Iowa 50011, USA

(Received 28 September 2005; revised manuscript received 30 March 2006; published 27 July 2006)

The elucidation of the local atomic structure of a pseudomorphic film of Cu deposited on the five-fold surface of *i*-$Al_{70}Pd_{21}Mn_9$ using medium-energy ion scattering spectroscopy is reported. Monte Carlo calculations, using the VEGAS code, have been utilized to simulate the blocking of 100 keV He^+ ions scattered from the overlayer. The coordinates of the Cu atoms in the overlayer derived from this procedure are consistent with a structure occurring in five rotational domains. Each domain consists of nanoscale strips of fcc Cu(100) with the ⟨110⟩ azimuth aligned along the five-fold directions of the quasicrystalline substrate. The strips are arranged according to a one-dimensional Fibonacci sequence with long and short widths related by the golden mean τ. Upon annealing the film transforms to an alloyed structure composed of five orientational domains of fcc material with the (110) axis perpendicular to the surface.

DOI: 10.1103/PhysRevB.74.035429 PACS number(s): 61.44.Br, 68.35.Bs, 68.37.Ef

I. INTRODUCTION

Few occurrences have had such an impact on the scientific community as the reporting in 1984 of a "metallic phase with long-range order and no translational symmetry".[1] The appearance within a rapidly quenched Al-Mn alloy of a phase possessing icosahedral symmetry forced a redefinition of what constitutes crystalline ordering to allow the inclusion of those materials we now refer to as quasicrystals.[2] Although the Al-Mn phase had a metastable structure, many thermodynamically stable quasicrystals have since been discovered, making possible the production of large, highly perfect single grains suitable for studies aimed at determining the structure and properties of these complex materials. The thermodynamically stable classes of quasicrystal are ternary compounds, with the one exception thus far known of $Cd_{5.7}Yb$. This complicates studies of the physical structure and the formation of quasicrystals a great deal, and has resulted in much effort being expended towards the formation of less chemically complex systems that still exhibit the aperiodic ordering which is of interest.[3–10]

One route to this end involves the use of quasicrystal surfaces as templates for the growth of epitaxial films which will reflect the aperiodic ordering present within the substrate. Within the constraint of the film having some property in common with the substrate, there are three possible growth modes. A film may grow in the "rotational epitaxy" mode, forming islands which follow rotational ordering in some way already present on the surface, but with each island composed of a usual crystalline form of the adsorbate, as reported for Ag and Al deposited on *i*-Al-Pd-Mn.[8–10] Alternatively, individual atoms or clusters may nucleate at specific sites on the quasicrystal surface, forming up to a monolayer of material with true quasicrystalline symmetry, as for Al adsorbed on *i*-Al-Cu-Fe, and Bi and Sb deposited on *i*-Al-Pd-Mn and *d*-Al-Ni-Co.[3,4] This is a "pseudomorphic" growth mode, in which the adsorbed atoms assume the icosahedral structure of the template completely. Finally, there is the possibility of the formation of a multilayer film which displays a balance between the natural crystalline structure of the material used, and the aperiodic nature of the quasicrystalline substrate (*i*-$Al_{70}Pd_{21}Mn_9$-Cu and *d*-$Al_{72}Ni_{11}Co_{17}$-Co);[5,6] this is also a pseudomorphic growth mode, and the structure of the film will necessarily be different from the usual bulk elemental structure.

The *i*-$Al_{70}Pd_{21}Mn_9$-Cu film was first studied using a scanning tunnel microscope (STM).[5] A five-domain row structure was observed in that study with the rows having long and short separations $L=7.3$ Å and $S=4.5$ Å and the sequence of the rows being quasiperiodic. A step height of 1.9 Å was also measured. A further study proposed a model for this structure based on the STM measurements and on LEED observations of periodicity along the row directions.[15] In this model, the rows observed in the STM images were modeled as "strips" of fcc(100) Cu of different widths L and S, arranged in a way consistent with the terms of the Fibonacci sequence and with each strip consisting of several atomic rows aligned along high symmetry directions of the substrate. For clarity, this nomenclature has been adopted in this manuscript.

This paper reports on a study of this film, with a view to testing of the previously proposed model and alternative models with a quantitative structural technique. Medium-

energy ion scattering (MEIS) is an extremely powerful tool for the elucidation of the structure and composition of the surface and near-surface regions. Quantitative information on the composition as a function of depth in the near-surface region can be found from energy-resolved spectra, and the positions and relative intensities of blocking dips in the angle-resolved spectra offer important information about the local atomic structure of the surface layers. In a previous paper we reported the first use of MEIS to characterize a clean quasicrystal surface[11] under a range of preparation conditions. The structure of the *i*-$Al_{70}Pd_{21}Mn_9$-Cu film is studied both "as-deposited" and after subsequent annealing to 600 K.

II. EXPERIMENTAL DETAILS

Data were obtained using the UK national MEIS facility at the CCLRC Daresbury Laboratory.[12] In this technique, the intensity of scattered He^+ ions of primary energy 100 keV is measured using a toroidal electrostatic analyzer with a position-sensitive detector, allowing simultaneous collection of scattered ions over a range of angles and energies. For each data set, a series of two-dimensional scans may be tiled together electronically to produce the final spectrum where the scattered ion intensity is represented by a false color scale. These two-dimensional spectra may then be projected onto either an energy scale, from which compositional data may be deduced, or onto an angle-resolved scale, from which information on the structure may be obtained.

The *i*-$Al_{70}Pd_{21}Mn_9$ sample was grown in the Ames Laboratory using the Bridgman method. Following alignment using back-reflection Laue diffraction, the sample was cut by spark etching perpendicular to a five-fold (100100) axis. Prior to insertion into an UHV, the quasicrystal was polished with successively finer grades of diamond paste (down to 0.25 μm). This procedure gives an optimal starting point for the subsequent *in situ* preparation, which consisted of cycles of Ar ion bombardment and subsequent annealing to a temperature of 950 K up to a total annealing time of 20 h. These preparation conditions have been found to give a flat surface with micron-scale terraces.[13,14]

Copper was evaporated with the chamber at a pressure of 1×10^{-9} mbar, using a resistively heated wire wrapped around a rod of oxygen-free high purity Cu. The sample was at room temperature during Cu evaporation, and the Cu source had been thoroughly degassed. Low-energy electron diffraction (LEED) was used to monitor the approximate coverage of Cu on the surface, showing the disappearance of the clean surface five-fold pattern and then the emergence of the tenfold pattern associated with the aperiodic Cu film.[15] Once the film had been formed on the surface, the sample was transferred to the analyzing chamber (base pressure 10^{-10} mbar) for the scattering experiments. The two-dimensional MEIS data were taken using an incidence of 31.8° with respect to the surface normal, which equates to a threefold axis orthogonal to a (1,1,1,1,1,1) type plane. For a description of the notation system see, e.g., Ref. 16. Each individual scan was collected for a fixed ion fluence of 2.5×10^{15} ions cm^{-2}, and the sample was moved between scans to minimize beam-induced damage.

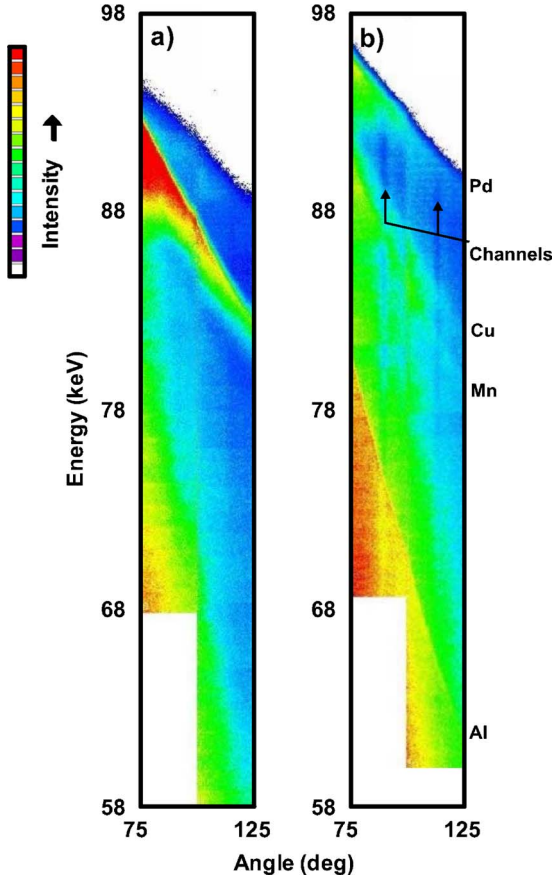

FIG. 1. (Color online) (a) Two-dimensional data obtained from the unannealed *i*-$Al_{70}Pd_{21}Mn_9$ surface after deposition of 9 ML of Cu. (b) Similar dataset after annealing the Cu film in (a) to 600 K for 10 min. The scattering features from the four elemental components of different mass and some characteristic quasicrystalline channels are indicated.

III. RESULTS AND DATA ANALYSIS

A. Unannealed Cu film

Figure 1(a) shows a two-dimensional data set taken from the *i*-$Al_{70}Pd_{21}Mn_9$ sample after the deposition of approximately 9 ML of Cu (calibrated using the energy-resolved data, see below). Diagonal bands of intensity can be seen, arising from a particular element and separated by energy, due to the increased energy transferred when an ion is scattered by an atom of lower mass. In addition, features of lower intensity can be seen running down the data set. These are blocking directions through the quasicrystal characteristic of the icosahedral ordering present.

An energy-resolved spectrum collected from this film is shown in Fig. 2(a). The data were fitted using the SIMNRA5.0 energy spectrum simulation code.[17] The fit involves components for both the surface, where complete illumination of the atoms occurs, and for a near-surface region starting directly below the surface and extending to the whole probing depth of the technique (around 500 Å). For the latter, reduced illumination is seen due to the fact that the energy spectrum is taken in a double alignment geometry and hence the atoms shadow each other.

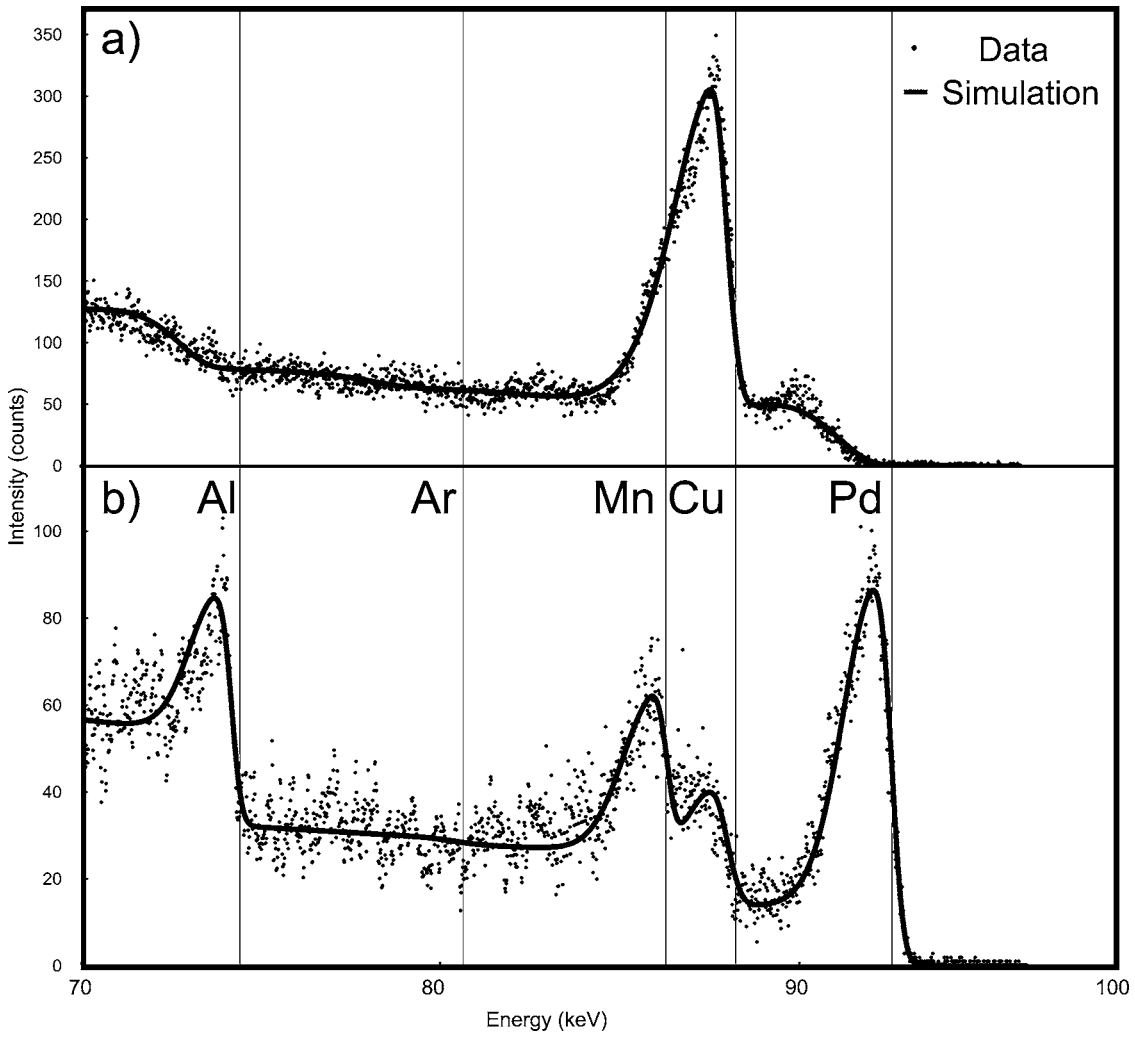

FIG. 2. One-dimensional energy-resolved data obtained from Cu/*i*-$Al_{70}Pd_{21}Mn_9$. (a) Spectrum from the unannealed film, showing a strong Cu signal and no surface peaks for the bulk components. (b) Spectrum from the annealed film, showing surface peaks for all elements present, indicating the alloying of the Cu with the surface of the quasicrystal.

The existence of a strong Cu surface peak and the lack of surface peaks for the bulk component indicates that the unannealed film does not alloy with the quasicrystal. The Cu coverage can be determined with a high degree of accuracy from the fitting code, and has been determined to be 18×10^{15} atoms cm^{-2}, which is equivalent to 9.5 ± 0.1 ML (from the density of bulk fcc Cu). Hereafter coverages will be quoted in monolayer equivalents (MLE). Below this is an Al-rich interlayer region, followed by an Mn-rich subsurface region, formed by the flat surface preparation process.[11] The fit also includes a small amount of Ar in the subsurface region. Buried Ar has been observed in these materials in a previous MEIS study[11] and arises from the sputtering procedure used to clean the sample. The compositions of the surface, interlayer, and subsurface regions, corrected for the visibility of each element in the subsurface region are shown in Table I.

The blocking curve for the unannealed Cu film is shown in Fig. 3(a). The curve was obtained by integrating the Cu signal from the two-dimensional data and then projecting it onto the angle axis. The signal from just above the Cu peak

TABLE I. The table shows compositional values in percentages for the unannealed and annealed films as determined from the energy-resolved data. For the unannealed film, the thickness of the surface Cu layer was 19×10^{15} at. cm^{-2} (9.5 monolayer equivalents) and that of the Al-rich interlayer was 10×10^{15} at. cm^{-2} (5 monolayer equivalents). For the annealed film, the thickness of the surface layer was 13×10^{15} at. cm^{-2} (6.5 monolayer equivalents).

		Surface (%)	Interlayer (%)	Subsurface (%)
Unannealed film	Cu	100	0	0
	Al	0	84	78
	Pd	0	11	10
	Mn	0	5	12
Annealed film	Cu	8		3
	Al	65		77
	Pd	11		7
	Mn	16		13

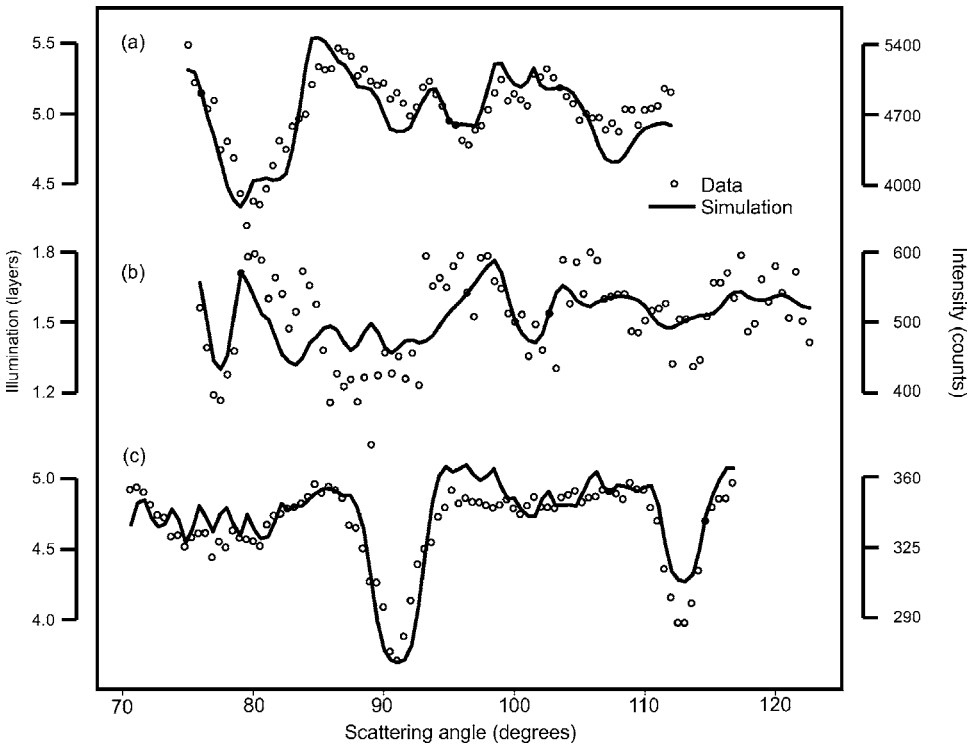

FIG. 3. (a) One-dimensional angle-resolved Cu data obtained from Cu/*i*-$Al_{70}Pd_{21}Mn_9$. (b) Annealed to 600 K for 10 min. (c) Clean surface Pd data for *i*-$Al_{70}Pd_{21}Mn_9$.[11] Scales for both intensity (counts) and illumination (layers) are shown.

was also taken and subtracted from the data, in order to provide a background correction. In this way features from the subsurface Pd blocking behavior may be removed from the Cu data prior to fitting.

The angular data were modeled using the VEGAS code. Since the Cu film forms in five structurally equivalent domains (as demonstrated by the previous studies[5,15]) single domain models were constructed and simulations were run in five azimuthal rotations and averaged to build up the final spectrum. Because a pentagon has five-fold symmetry along the appropriate axes, orientations that are opposite according to the line of symmetry can be considered equivalent, reducing the number of simulations needed to three per structural model. The interaction of the beam with the model structures could then be simulated for three inequivalent azimuthal orientations and the blocking curves averaged with 1:2:2 weighting to provide the final simulated spectrum. In the models, each domain is composed of strips of material whose widths are arranged to follow a Fibonacci sequence of long and short distances. The structure of the individual strips was modeled as conventional crystalline material using several alternative low index planes parallel to the surface, in a number of alternative rotational orientations with respect to the substrate.

Fitting of the blocking curves was carried out initially considering a structure with fcc(110) termination within the strips, since this orientation has been observed previously in cubic films found on quasicrystal surfaces[18] (and indeed matches that of the film formed on annealing the Cu structure—see Sec. III B). These attempts were unsuccessful. The (311) orientation (also observed when sputtering *i*-$Al_{70}Pd_{21}Mn_9$) and close-packed fcc(111) and hcp(0001) orientations were also tried. However, none of these structures gave a reasonable fit to the experimental data, which could only be achieved using an fcc(100) termination within the strips, with a ⟨110⟩ azimuth aligned to the five-fold directions of the quasicrystalline substrate. The model is shown in Fig. 4.

As in the LEED model, the strips were modeled using random offsets. The offsets could be interpreted as a reflection of the positioning of the "dark star" five-fold hollow nucleation sites observed on the clean surface.[19] However, any attempt to model this quasiperiodic ordering, either by using offsets generated from positions of Mn atoms in an ideal clean model surface or interpenetrating Fibonacci grids oriented at 72° to each other failed to improve the fit.

Different dimensions of the model were considered to optimize calculation time without sacrificing accuracy taking into account the fact that the computation time directly scales with model size. A previous treatment of clean surface MEIS data[11] involved the use of a large (~4000 atom) cuboidal section of the accepted bulk icosahedral structural model as an approximation to the *i*-$Al_{70}Pd_{21}Mn_9$ surface. A model of comparable size was not considered necessary in this case, as the Cu does not exhibit icosahedral structure, but is aperiodic in one dimension only. Hence the model is extended along only one dimension and, as explained above, rotated through

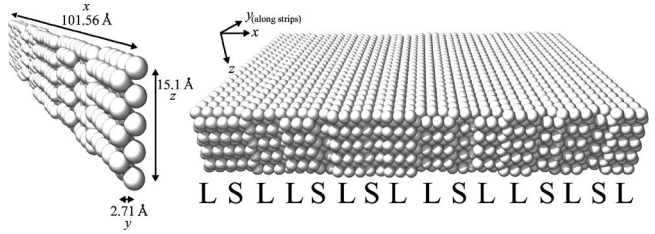

FIG. 4. The best-fit model as run. Also shown is an extension of the model into one 100×60×15 Å domain.

pentagonal angles in order to build up a spectrum for the five observed domains. The length of the model in the aperiodic direction (y) was chosen to be around 100 Å, since below this value varying the length altered the character of the simulated curve. The height of the model in the direction perpendicular to the surface (z) was 9 MLE, according to our measured average film thickness assuming the film density to be the same as that of bulk Cu. The length of the model parallel to the strips (y) was equal to the repeat distance, which in the case of an unstrained model would be the bulk nearest neighbor distance (2.56 Å).

The fits achieved using this model required a significant amount of disorder of around 30% to be added (using our previously established methodology[11]), and one potential reason for this was thought to be the effect of domain boundaries. For this reason calculations were performed for more complex models including one with ~14 000 atoms which included two domains. This work demonstrated that the number of atoms near domain boundaries is not large enough to produce any additional blocking features or have any other significant effect on the spectra. Hence the domain boundaries cannot account for all the disorder seen. Another possibility to account for the fitted disorder would be unregistered atoms at the interface between the strips. However, the perfection of the strip pattern seen in the STM images might suggest that this is unlikely. The disorder is most likely to arise from sources that could equally be seen for normal crystalline films, including defects such as interstitial atoms in the fcc substructure and/or areas of amorphous material distributed over the macroscopic surface.

In the best-fit model, Cu atoms are arranged with the fcc nearest neighbor distances running in-plane both parallel (y) and perpendicular (x) to the strip pattern. This gives rise to three atomic rows in the short strips (width 4.561 Å) and five atomic rows in the long strips (width 7.379 Å). In order to further improve the fit, the atomic separations were varied in all three dimensions (x, y, and z). In the best-fit model the separation of the Cu atoms parallel to the strip pattern (y) was increased from 2.56 Å to 2.71±0.02 Å. While the separation perpendicular to the strip pattern (x) remained at bulk values, the separation in height (z) was adjusted from 1.81 to 1.67 Å to maintain film density at the bulk value.

B. Annealed Cu film

Figure 1(b) shows a two-dimensional data set taken after annealing the Cu film described in Sec. III A to 600 K for 10 min. An energy resolved spectrum from the annealed film is shown in Fig. 2(b). Strong surface peaks from all the elements are present. This compositional profile is well matched using a two-layer model comprising the alloy film and a bulklike subsurface region. The fit also included a small amount of Ar in the subsurface region, as discussed above. The compositions of the surface and subsurface regions, corrected for the visibility of each element in the subsurface region, are again shown in Table I.

From the energy spectra presented in Fig. 2 it is clear that the total amount of Cu in the film has been dramatically reduced after annealing to 600 K for 10 min. The composition and thickness data shown in Table I demonstrate that the total Cu content in the quaternary alloy film has dropped from 18×10^{15} at. cm^{-2} to 1×10^{15} at. cm^{-2}, a loss of 95%. Since the annealing temperature was relatively low the vapor pressure of Cu would be negligible and reevaporation can be ruled out as a mechanism for the loss. The fit presented in Fig. 2(b) includes Cu running through the near surface region at a level of approximately 3%. However, the subsurface signal between 75 and 85 keV has contributions from Mn, Cu, and Pd. While the Pd contribution is fixed by the signal seen in front of the Cu peak, there is a great deal of uncertainty in the relative proportions of the Mn and Cu present. In addition to the composition of the surface and near-surface layers, the SIMNRA fit also includes a parameter for surface roughness, which effectively smears the interface between the two layers of the model. This parameter can account for not only surface roughness but also interfacial roughness and, as may well occur in this case, a gradually changing composition between the layers at the interface. Hence the composition profile is largely consistent with that expected for classic Fickian diffusion and hence we suggest this is the most likely mechanism for Cu loss.

The blocking curve for the annealed Cu film is shown in Fig. 3(b). The blocking curve was best simulated using five domains of fcc material with (110) planes perpendicular to the surface and ⟨110⟩ azimuths oriented along the fivefold directions of the substrate. Two parameters were adjusted to optimize the fit. The first of these was disorder, which was accounted for by mixing the simulation with flat signal. The resulting fit of 6.7±5.9% implies a high level of crystallinity in the quaternary alloy film. The other parameter incorporated into the fit was perpendicular strain with the best fit arising for a value of 6.9±2.1%. Due to the low percentage of Cu in this alloy film, the statistics are less good for this fit.

IV. DISCUSSION

A. Unannealed Cu film

The previous LEED analysis[15] yielded a Cu nearest neighbor distance of 2.5±0.1 Å. Although not in perfect agreement with the MEIS value of 2.71±0.02 Å, the combined findings do provide strong evidence for this structural model. It is noteworthy that in the stereographic projection for the fcc(100) surface (reproduced in Fig. 5), there is a line of high symmetry at 71.57°. An extension of 2.5% in one direction of the lattice allows this line to fall at 72°, which is a pentagonal angle. Indeed this orientation is responsible for the primary features seen in the blocking curve as demonstrated by the three individual curves which, when averaged together, make up the best-fit model and are also shown in the figure. This supports the idea of an expansion rather than a contraction, and for Cu would mean a lattice expansion from 2.56 to 2.62 Å; we detect a lattice expansion of 5% from 2.56 to 2.71 Å. Reducing the spacing along the strips leads to a splitting of the blocking dip at around 80° which is inconsistent with the data. In order to maintain film density the spacing parallel to the surface (z) has been adjusted while the value perpendicular to the strips remained at bulk values. The lack of strain parallel to the surface and perpendicular to

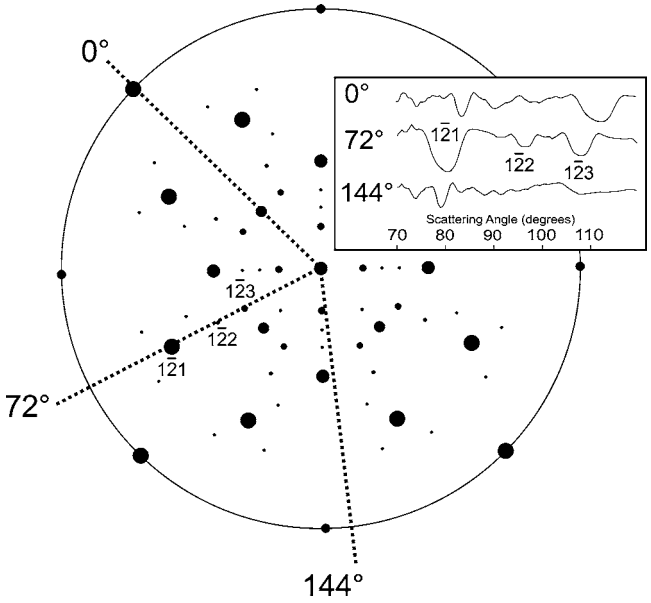

FIG. 5. Part of the stereographic projection for fcc, with pentagonal angles superimposed. Inset: The three azimuthal components of the best fit model. The blocking dips may be easily identified with directions on the stereographic projection.

the strips is perhaps not surprising since the breaks in the structure that occur at the strip edges could be viewed as a strain relieving mechanism.

The strip structure was apparent from the initial STM work on the system.[5] While the MEIS technique is likely to have some limited sensitivity to the average strip width, as indicated by the fact that simulations based on simple fcc structure do not fit the data well, the sensitivity of the technique was not further tested in this work because the information was so readily available from the STM images. MEIS is far more sensitive to the local atomic structure within each nanoscale strip. The long and short separations (7.3 and 4.5 Å) seen in the STM images were in good agreement with separations of a number of features in typical surface terminations of the ideal bulk structure. The "dark stars" apparent in STM images of the clean i-$Al_{70}Pd_{21}Mn_9$ surface have these separations and have been shown to be nucleation sites for other adsorbates.[19] The theoretical work of Krajčí *et al.*[20] also suggests that these may be candidate sites for the nucleation of the Cu structure. Manganese atoms in the surface layer also have similar separations. However, even if the "dark star" features are responsible for nucleation of the Cu film, only a few atoms in the proposed structure sit in well defined sites and hence the MEIS data would be relatively insensitive to this since no new features would be expected in the surface blocking curves of the substrate.

In some ways the structure of this film is similar to the quasiperiodic row structure found for Ag films grown on GaAs(110).[21,22] However, there are two important differences. The principal difference is that the quasiperiodic row structure of GaAs(110)-Ag is a surface modulation confined to the top few angstroms of a Ag(111) film. In this study the strip structure is confirmed to be present throughout the whole depth of the film. The second difference is the registry between the rows, which in the case of the Ag/GaAs system is periodic, but in the current study has been modeled using random offsets.

B. Annealed Cu film

The angle-resolved data presented in Fig. 3(b) clearly demonstrate the structural transformation of the film. By comparison with simulations it can be seen that this new structure involves five domains of fcc material with (110) termination. In fact, this termination is commonly seen for crystalline phases formed on the five-fold surface of i-$Al_{70}Pd_{21}Mn_9$ after sputtering.[10,19] Both cubic close packing and icosahedral structure are densely packed arrangements. The (111) cubic surface and the icosahedral three-fold surface involve triangular arrays of atoms which, when aligned together lead to a near coincidence of cubic (110) planes with icosahedral five-fold axes and hence, this is a favored epitaxial arrangement of the two structures. This epitaxial arrangement is discussed in considerably more detail by Shen *et al.*[18]

The origin of the perpendicular strain in this film is not clear since no detailed understanding of the interface between the film and substrate has been achieved. However, in the case of the AlPd(110) film formed when i-$Al_{70}Pd_{21}Mn_9$ is sputtered, which has a lattice parameter of 3.03 Å, no strain is observed.[11] If the interface of this quaternary alloy phase with the icosahedral substrate is basically similar to the sputtered phase, then the fitted strain would imply a larger lattice parameter of approximately 3.1 Å. While this value is smaller than the lattice parameter of any of its constituent pure metals this is not uncommon for metal alloys as demonstrated by the lattice parameter of AlPd which is itself somewhat smaller than that of either Al or Pd in elemental form.

V. CONCLUSIONS

The structure of a pseudomorphic thin Cu film grown on the five-fold surface of i-$Al_{70}Pd_{21}Mn_9$ consists of five rotational domains of a one-dimensional Fibonacci array of strips whose widths are τ-scaled distances characteristic of the quasicrystal surface (L=7.379 Å and S=4.561 Å). This work has demonstrated that the strips are composed of fcc material with the (100) direction oriented perpendicular to the surface and nearest neighbor distances running both parallel and perpendicular to the strip pattern. The fcc material is distorted so that the nearest neighbor distance along the strips is 2.71±0.02 Å, with a corresponding compression perpendicular to the surface resulting in a step height of 1.67±0.02 Å. This quantitative structural characterization of this film provides independent confirmation of a previously proposed structural model.

Annealing the room temperature grown Cu film to 600 K for 10 min led to the diffusion of Cu into the substrate leaving a quaternary alloy at the surface. This alloy has a fcc(110) structure similar to that found in the fcc Al-Pd film formed when i-$Al_{70}Pd_{21}Mn_9$ is sputtered.

ACKNOWLEDGMENTS

The authors wish to thank Renee Diehl of the Pennsylvania State University for valuable discussions regarding the fitting of the angle-resolved data using the VEGAS code. This material is based upon work supported by the EPRSC under Grants No. GR/S19080/01 and No. GR/R88809/01 providing direct access to the MEIS facility. The Austrian Science Fund (FWF) is acknowledged for financial support (Project No. J2417-NO8). The FOM Institute, Amsterdam is thanked for providing the VEGAS code.

---

*Present address: LSG2M, CNRS UMR 7584, Ecole des Mines, Parc de Saurupt, 54042 Nancy Cedex, France.

[1] D. Shechtman, I. Blech, D. Gratias, and J. W. Cahn, Phys. Rev. Lett. **53**, 1951 (1984).

[2] International Union of Crystallography, Acta Crystallogr., Sect. A: Found. Crystallogr. **48**, 928 (1992).

[3] T. Cai, J. Ledieu, R. McGrath, V. Fournée, T. A. Lograsso, A. R. Ross, and P. A. Thiel, Surf. Sci. **526**, 115 (2003).

[4] K. J. Franke, H. R. Sharma, W. Theis, P. Gille, P. Ebert, and K. H. Rieder, Phys. Rev. Lett. **89**, 156104 (2002).

[5] J. Ledieu, J.-T. Hoeft, D. E. Reid, J. A. Smerdon, R. D. Diehl, T. A. Lograsso, A. R. Ross, and R. McGrath, Phys. Rev. Lett. **92**, 135507 (2004).

[6] J. A. Smerdon, J. Ledieu, J. T. Hoeft, D. E. Reid, L. H. Wearing, R. D. Diehl, T. A. Lograsso, A. R. Ross, and R. McGrath, Philos. Mag. **86**, 841 (2006).

[7] J. Ledieu, R. McGrath, R. D. Diehl, T. A. Lograsso, A. R. Ross, Z. Papadopolos, and G. Kasner, Surf. Sci. Lett. **492**, L729 (2001).

[8] V. Fournée and P. A. Thiel, J. Phys. D **38**, R83 (2005).

[9] B. Bolliger, V. E. Dmitrienko, M. Erbudak, R. Lüscher, H.-U. Nissen, and A. R. Kortan, Phys. Rev. B **63**, 052203 (2001).

[10] V. Fournée, T. C. Cai, A. R. Ross, T. A. Lograsso, J. W. Evans, and P. A. Thiel, Phys. Rev. B **67**, 033406 (2003).

[11] T. C. Q. Noakes, P. Bailey, C. F. McConville, C. R. Parkinson, M. Draxler, J. A. Smerdon, J. Ledieu, R. McGrath, A. R. Ross, and T. A. Lograsso, Surf. Sci. **583**, 139 (2005).

[12] P. Bailey, T. C. Q. Noakes, and D. P. Woodruff, Surf. Sci. **426**, 358 (1999).

[13] J. Ledieu, A. W. Munz, T. M. Parker, R. McGrath, R. D. Diehl, D. W. Delaney, and T. A. Lograsso, Surf. Sci. **433/435**, 665 (1999).

[14] J. Ledieu, A. W. Munz, T. M. Parker, R. McGrath, R. D. Diehl, D. W. Delaney, and T. A. Lograsso, Mater. Res. Soc. Symp. Proc. **553**, 237 (1999).

[15] J. Ledieu, J. T. Hoeft, D. E. Reid, J. A. Smerdon, R. D. Diehl, N. Ferralis, T. A. Lograsso, A. R. Ross, and R. McGrath, Phys. Rev. B **72**, 035420 (2005).

[16] C. Janot, *Quasicrystals, A Primer* (Oxford Science Publications, Oxford, 1992), p. 187.

[17] M. Mayer, "SIMNRA Users Guide" Report IPP 9/113, Max-Planck-Institute fur Plasmaphysik Garching, Germany, 1997.

[18] Z. Shen, M. J. Kramer, C. J. Jenks, A. I. Goldman, T. A. Lograsso, D. Delaney, M. Heinzig, W. Raberg, and P. A. Thiel, Phys. Rev. B **58**, 9961 (1998).

[19] J. Ledieu and R. McGrath, J. Phys.: Condens. Matter **15**, S3113 (2003).

[20] M. Krajčí and J. Hafner, Phys. Rev. B **71**, 054202 (2005).

[21] A. R. Smith, K.-J. Chao, Q. Niu, and C.-K. Shih, Science **273**, 226 (1996).

[22] P. Ebert, K.-J. Chao, Q. Niu, and C. K. Shih, Phys. Rev. Lett. **83**, 3222 (1999).